Effect of electrostatic interactions on the structure and dynamics of a model polyelectrolyte. II. Intermolecular correlations

ARTICLE *in* THE JOURNAL OF CHEMICAL PHYSICS · JANUARY 1999

Impact Factor: 2.95 · DOI: 10.1063/1.477887

Effect of electrostatic interactions on the structure and dynamics of a model polyelectrolyte. II. Intermolecular correlations

Lidia Skibinska and Jacek Gapinski
Institute of Physics, Adam Mickiewicz University, Umultowska 85, 61-614 Poznan, Poland

Hui Liu
Department of Chemistry, Stanford University, Stanford, California 94305-5080

Adam Patkowski
Institute of Physics, Adam Mickiewicz University, Umultowska 85, 61-614 Poznan, Poland, and Max-Planck-Institut für Polymerforschung, Ackermannweg 10, 55128 Mainz, Germany

Erhard W. Fischer
Max-Planck-Institut für Polymerforschung, Ackermannweg 10, 55128 Mainz, Germany

R. Pecora[a)]
Department of Chemistry, Stanford University, Stanford, California 94305-5080

(Received 16 July 1998; accepted 14 October 1998)

The peak in the small angle x-ray scattering and the dynamic light-scattering slow mode for a 20 base-pair duplex oligonucleotide (''B-DNA'') are studied as functions of oligonucleotide and added-salt (NaCl) concentrations. Both the x-ray peak intensity and the relative intensity of the slow mode decrease as the added-salt concentration is increased. The hydrodynamic radius of the slow mode increases as the added-salt concentration is decreased. The x-ray peak gradually disappears with increasing salt while the slow mode decreases in intensity, but still has some residual intensity at the highest added-salt concentration studied. There is no abrupt change in either the peak or the slow mode with increasing salt. The existence and behavior of both the x-ray peak and the slow mode indicate local ordering in the solution due to electrostatic forces. The x-ray peak position for the oligonucleotide is correlated with the static light-scattering peak seen by other workers for dilute solutions of larger polyions. A simple model shows that the reduced electrostatic potential at the average distance between neighboring polyions is approximately the same for these polyelectrolytes. The slow mode has a hydrodynamic radius that increases with decreasing q at low added-salt concentrations, indicating a large correlation volume. The x-ray peak is a more local indicator of nearest-neighbor correlations among the polyions. [S0021-9606(99)50703-4]

I. INTRODUCTION

Oligonucleotides, in spite of their small size, have several characteristics that make them excellent model systems for studying polyelectrolyte dynamics. They are nearly monodisperse, have known molecular weights, and, at low molecular weights in their double helical B-form, are rigid and rod-like under a wide range of solution conditions. In a preceding article (hereafter referred to as I),[1] we presented the results of dynamic light-scattering photon correlation spectroscopy and depolarized Fabry–Perot interferometry experiments on a 20 base-pair duplex oligonucleotide (''B–DNA''). The dynamic light-scattering photon correlation spectroscopy time-correlation functions of this oligonucleotide, as well as those of longer DNAs[2–10] and other polyelectrolytes, show a mode usually attributed to coupled polyion–small ion diffusion and a ''slow mode'' whose molecular origin is still a matter of controversy.[11–17] The slow mode generally increases in prominence as the concentration of salt is decreased and that of the polyion is increased. In addition, a peak has been observed in the small-angle x-ray (SAXS)[18–21] and small-angle neutron (SANS)[10] scattering from DNA as well as from other polyelectrolyte solutions. The position of this peak depends on the concentration of the polyion. It is very prominent at low salt conditions and gradually becomes less distinct as the salt concentration is raised. It is a matter of controversy as to whether or not the peak position depends significantly on the salt concentration.[10,18–21]

In I, we presented and discussed experimental results on the salt concentration and polyion concentration dependencies of the translational (photon correlation spectroscopy fast mode) and rotational (depolarized Fabry–Perot interferometry) motions in this well-defined system. In this article, we focus on the slow mode observed in the photon correlation spectroscopy time-correlation functions and on the peak in the SAXS scattering from this same system. Only a few studies have combined these techniques to study a common system. The earliest is the photon correlation and SAXS experiments of Patkowski *et al.* on t–RNA.[18] More recently, Bloomfield and co-workers[7,19] have performed photon corre-

[a)]Author to whom correspondence should be addressed.

lation spectroscopy and SAXS experiments on persistence-length DNA, while Borsali *et al.* have performed SANS scattering and photon correlation spectroscopy on a DNA sonication fragment.[10] Of these, only t–RNA is as well defined in terms of molecular weight and monodispersity as the 20-mer studied here.

In Sec. II, we briefly describe the experimental protocols and in Sec. III, we present and discuss the small-angle x-ray scattering experiments and the photon correlation spectroscopy slow-mode results. Section IV summarizes our correlations.

II. EXPERIMENT

A. Sample preparation and DLS–photon correlation spectroscopy

The sample preparation and light-scattering apparatus are described in detail in I.[1] Briefly, the sample is a 20 base-pair synthetic duplex oligonucleotide with the primary structure: **5′–CGT ACT AGT TAA CTA GTA CG–3′**. The DNA was purchased from the Midland Certified Reagent Company, Midland, Texas, catalog #CO-1000, lot #061394-283. It was synthesized by the phosphoramidite chemistry method and purified by anion-exchange high-pressure liquid chromatography. After purification, the pooled fractions were desalted by gel filtration. The product was supplied as the lyophilized sodium salt of DNA. The oligonucleotide is of greater than 99.9% monodispersity, as verified by capillary gel electrophoresis with detection by ultraviolet absorption at 260 nm. Solutions were prepared as described in I. The buffers used contained 10 mM Tris to maintain solution *p*H at 7.6, and various amounts of added NaCl to achieve different solution ionic strengths. All buffer solutions (except those denoted ''no added salt'') also contained 1 mM EDTA to chelate any trace amounts of multiply charged ions. DLS–photon correlation spectroscopy equipment at Stanford, Mainz, and Poznan was used for the measurements. In each of these three cases, a logarithmic correlator was used to compute the light-scattering intensity time-correlation functions. The use of logarithmic correlators is important for easy separation of the slow mode from the fast mode that was analyzed in detail in I. Data were analyzed using the CONTIN program,[22] as well as by double exponential fits. The CONTIN program recovers the distribution of relaxation times without prior knowledge of the number of relaxation processes. Results from all three laboratories were consistent. Most studies of the slow mode were done at scattering angles of 90°, although some were done at lower scattering angles.

B. Small-angle x-ray scattering

The small-angle x-ray scattering measurements were made with a Kratky Compact camera (A. Paar, KG) equipped with a one-dimensional position-sensitive detector (N. Braun). The Ni-filtered CuK_α radiation was used from a Siemens generator (Kristalloflex 710H) operating at 35 kV and 30 mA. The intensity data at a scattering vector q [$=(4\pi/\lambda)\sin(\theta/2)$, where λ is the x-ray wavelength and θ is the scattering angle] were collected in a multichannel analyzer (PC card, Silena) and stored for further analysis. The q range investigated was from about 0.14 to 3.7 nm^{-1}. Data treatment involved corrections for absorption, background scattering, and slit-length smearing. Primary beam intensities were determined by the moving slit method.

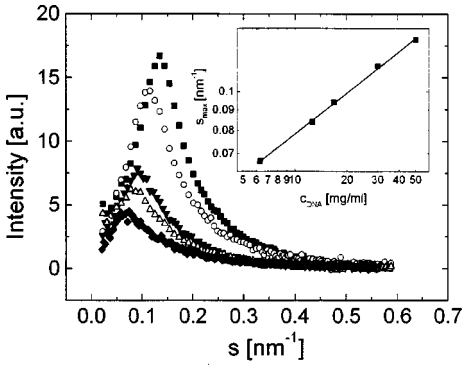

FIG. 1. SAXS intensities vs oligomer concentration at no added salt concentration. The curves correspond to the following DNA concentrations: (top to bottom): 50, 30, 16.7, 12.6, and 6.3 mg/ml. The inset shows a log–log plot of the peak position vs DNA concentration.

III. RESULTS AND DISCUSSION

A. Small-angle x-ray scattering (SAXS)

A well-defined peak in the x-ray scattering appears at all oligonucleotide concentrations studied at low and moderate concentrations (up to 100 mM) of NaCl. Figure 1 shows the SAXS intensity versus scattering number s ($s=q/2\pi$ where q is the scattering-vector length) for the sample in Tris buffer without EDTA and without added salt at various oligonucleotide concentrations. The peak maximum positions (s_{max}) plotted as a function of DNA concentration fall on a straight line on a log–log plot as seen in the inset in Fig. 1. The slope of the line, equal to 0.34 ± 0.01, within the experimental error corresponds to the simple relation $s_{max}\propto(c_{DNA})^{1/3}$. A plot of the peak position vs the cube root of the oligonucleotide number concentration is shown in Fig. 2. The slope of the line for our data is 1.

These results correspond to what one expects from a system with strong correlations between nearest neighbors at a distance $1/s_{max}$ apart. This length is often called the ''Bragg distance'' because of the similarity to Bragg's rela-

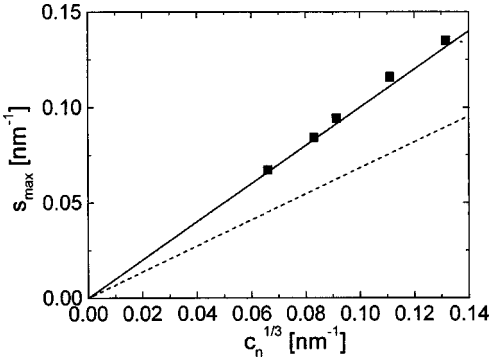

FIG. 2. SAXS peak positions vs $c^{1/3}$. The solid line is a linear fit to the data points. The theoretical prediction of Koyama (Ref. 23) for dilute strong polyelectrolyte solutions with no added salt is also shown (dashed line).

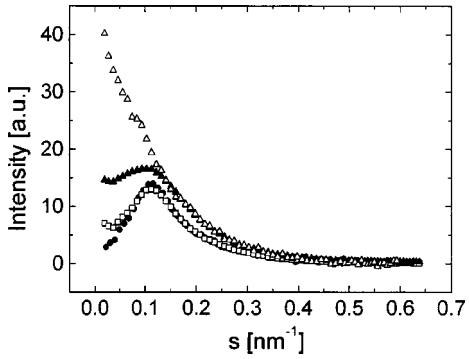

FIG. 3. SAXS profiles vs reduced wave vector for the 20-mer at the concentration of 30 mg/ml measured for various salt concentrations (full circles—0, open squares—10, full triangles—100, open triangles—500 mM).

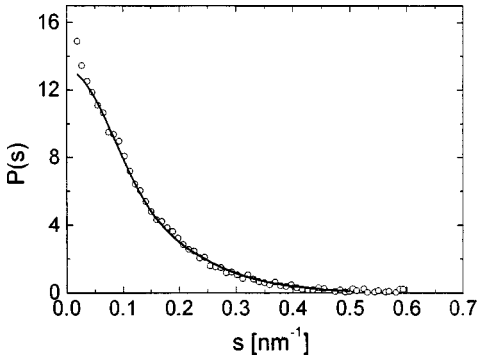

FIG. 4. Particle-scattering factor of the 20-mer calculated using the method of Diaz *et al.* (Refs. 24,25). The experimental SAXS data for a solution at 30 mg/ml oligomer concentration and 500 mM salt are also shown.

tion for an ordered system. The other line in Fig. 2 corresponds to Koyama's theoretical prediction (slope 0.632) for a dilute strong polyelectrolyte with no added salt.[23] Koyama's model essentially assumes an ''excluded volume'' about each polyion. Our results and those of Patkowski *et al.*[18] and Wang and Bloomfield[19] in their lower concentration range do not agree with Koyama's model. Note that our system is well below c^*, the overlap (or ''entanglement'') concentration defined for rigid rod systems as $c^* = 1/L^3$. For the 20 base pair oligonucleotide, $c^* = 69$ mg/ml. Our highest concentration studied is 50 mg/ml.

Figure 3 shows the SAXS profiles for samples with different added salt amounts at a constant DNA concentration of 30 mg/ml. The influence of the salt is already visible in the 10 mM NaCl sample as a slight broadening of the peak. Further increase of the salt concentration makes the peak more flat, especially on the low s side. Finally, the peak totally disappears at a few hundred mM NaCl.

Within the error of the measurements, the peak position does not change with salt concentration. Borsali *et al.*[10] find the SANS peak position from a longer, more concentrated DNA solution to be insensitive to salt. Wang and Bloomfield[19] find their SAXS peak position to be salt dependent for persistence length DNA. Koch *et al.*[20] find only a weak dependence on salt. The peak, in any case, is correlated with the electrostatic forces and its strength varies in a continuous manner. There does not appear to be an abrupt transition.

We have calculated the particle form factor, $P(s)$, for an isolated oligonucleotide molecule using the procedure of Garcia de la Torre *et al.*[24] In this procedure, the oligonucleotide is modeled as a rigid double helix with the usual DNA parameters, with each nucleotide represented by a sphere. In our case, the 20-mer is modeled as a set of 40 beads placed at the geometrical centers of the individual nucleotides. The bead radii are set such that all atoms fall within the beads. The form factor is then calculated as a superposition of sphere structure factors.[25] The result is shown in Fig. 4, along with the experimental SAXS curve for the highest salt concentration studied (500 mM NaCl), where electrostatic interactions are expected to be minimal. The agreement is excellent.

The relation between the measured scattered intensity and the form and solution structure factors for a system of monodisperse spherical particles is

$$I(s) \propto P(s)S(s). \tag{1}$$

Equation (1) is, in general, not valid for asymmetric particles like those considered here. It may, however, be a good approximation at dilute oligonucleotide concentrations, where orientational correlations between the 20-mers might be small. In any case, we show in Fig. 5, the $S(s)$ obtained by dividing the observed x-ray intensities by $P(s)$. The peaks of $S(s)$ defined in this way become less distinct and move toward higher s. If we interpret the reciprocal of the peak position of $S(s)$ as corresponding to the nearest-neighbor peak in the radial distribution function of the rod centers, we find that the rod centers appear to be closer than the Bragg distances obtained from the peak of $I(s)$ and shown in Fig. 2. Thus, the distances derived in this manner are shorter than those between polyion centers in the random (uniform) distribution. This result could be an indication of the inapplicability of Eq. (1) to our system. Studies on less asymmetric polyions have, however, also indicated shorter distances.[26,27] Repulsive interpolyion forces would give a separation larger than the random distribution, as in that from Koyama's model shown in Fig. 2. Shorter distances may indicate the presence of attractive forces.[26–31] Given the uncertainties in the applicability of Eq. (1), and the further difficulty in determining the peak positions in $S(s)$ when applying it to our data (Fig. 5), more quantitative statements on this issue cannot be made.

In I, we showed that the rotational relaxation times of the oligonucleotide at low added salt conditions slowed down strongly as the concentration of 20-mer was increased. This slowing down could result from orientational correlations between oligonucleotides. Furthermore, if effective dimensions of DNA that take into account electrostatic interactions are used, our solutions may no longer be considered dilute. For instance, in I, we estimate that c^* calculated using effective dimensions is 11 mg/ml in the buffer with $c_s = 3$ mM rather than $c^* = 69$ mg/ml estimated from DNA structural parameters. By this criterion, many of the lower added salt solutions considered here would be in the semidi-

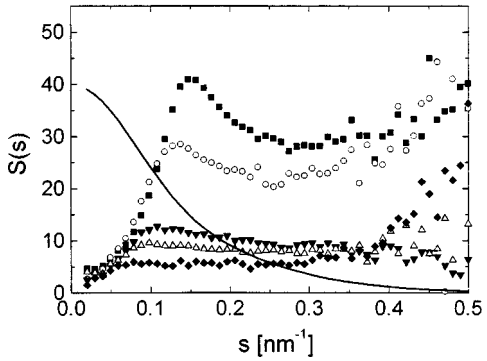

FIG. 5. Solution structure factor calculated according to Eq. (1), using an arbitrary proportionality constant. Note that the peaks move toward higher *s* relative to those in Fig. 1. The plot symbols correspond to those in Fig. 1. The calculated particle form factor is also shown (solid line).

lute region. The $c^{1/3}$ behavior of the peak position shown in Fig. 2, however, indicates dilute solution behavior.

There are very strong similarities between the *q*-dependence of static light scattering (SLS) data from very dilute solutions of high molecular weight polyelectrolytes and SAXS curves obtained for more concentrated (although still below the overlap concentration c^*) solutions of lower molecular weight polyelectrolytes. Using our data and SLS[12,13] and SAXS[18,26] data from the literature, we give a qualitative comparison of the two system types in terms of an assumed intermolecular pair potential. Our arguments indicate that the peaks observed in these systems arise from essentially the same molecular phenomenon: local (''domain'') ordering.

For our 20-mer under the conditions studied, $d=1/s_{\max}$, while for other polyelectrolytes it is often larger then $1/s_{\max}$. This is usually the case for long molecules like large sodium poly (styrenesulfonates) (NaPSS) molecules, probably because they are locally oriented, and the effect of the finite molecule length makes most of their ''bodies'' stay closer to one another than their centers. Similar effects occur at concentrations close to c^*. Entanglement results in an increase in the slope of $\log(s_{\max})$ vs $\log(c_p)$ from 1/3 to 1/2. Some of these features are presented in Fig. 6.

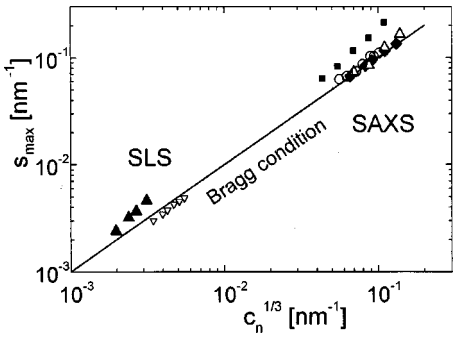

FIG. 6. Comparison between peak positions of SLS and SAXS data in solutions with no added salt. SLS: full triangles—NaPSS 7.8×10^5 from Drifford and Dalbiez (Ref. 12), open triangles—proteoglycan 1.16×10^6 from Li and Reed (Ref. 13), SAXS: full squares—NaPSS 7.4×10^4, open triangles—NaPSS 1.8×10^4 from Ise *et al.* (Ref. 26), open circles—*t*-RNA from Patkowski *et al.* (Ref. 18), full diamonds—20-mer from current work.

We analyze the strength and range of the electrostatic pair potentials. We use formulas for the electrostatic potential of charged spheres in the same manner as was done by Corti and Degiorgio for charged micelles.[32] The spheres are of radius *a*, charge *Z*, and a distance *r* apart. We use *x*, the reduced normalized distance, below

$$x=\frac{r-2a}{2a}. \tag{2}$$

The potential energy is for $\kappa a \ll 1$

$$V(x)=\frac{Z^2e^2}{2\varepsilon a(1+\kappa a)^2}\frac{\exp(-2\kappa a x)}{(1+x)}, \tag{3}$$

and for $\kappa a \gg 1$

$$V(x)=\frac{\varepsilon a \Psi_0^2}{2\ln[1+\exp(-2\kappa a x)]}, \tag{4}$$

where κ, the inverse Debye length, is given in terms of the salt concentration c_s and the charge on the salt coions *z*

$$\kappa^2=\frac{8\pi c_s e^2 z^2}{\varepsilon k_B T}, \tag{5}$$

and Ψ_0 is the surface potential

$$\Psi_0=\left(\frac{2k_BT}{e}\right)\sinh^{-1}\left[\frac{2\pi e\kappa^{-1}Ze}{4\pi a^2\varepsilon k_BT}\right]. \tag{6}$$

We first estimate the distances between molecules for the two regions, and also the inverse Debye screening lengths κ as functions of salt concentration. We assume equivalent spheres with radii roughly corresponding to those of the nonspherical systems studied: 20Å for SAXS and 200Å for SLS. We calculate $V(x)/k_BT$ for various assumed polyion charges. The results are shown in Figs. 7(a) and 7(b).

Comparison of these figures shows that the combination of ionic strength and charge that gives a similar reduced potential corresponds to the experimental condition in each case where a peak is seen. This indicates that the effect of the molecular charge in the SLS case easily compensates for the large interpolyion distance. An important difference between the two cases is the dependence of the potential on ionic strength. In the case of small molecules (and small distances), a change of ionic strength from 10^{-5} to 10^{-4} M causes only a five fold decrease of the potential, while in the other case the ratio is 100. We conclude from this that electrostatic interactions in high molecular weight polymer solutions decay at low ionic strength values. This statement is well supported by the SLS data of Li and Reed[13] (Fig. 4 in their paper), where the structure peak disappears for ionic strengths larger then 2×10^{-4} M.

We should note, however, that the potential used here is purely repulsive. It neglects the attractive van der Waals part that is likely not important at the distances considered and any possible attractive forces that might arise from fluctuations in the positions of the small ions.[27–31]

More information can be obtained from an analysis of the widths and amplitudes of the peaks. Since there is a large *q* range from the SLS to the SAXS regions, we have plotted all intensities as functions of *sd*, where *d* is the average dis-

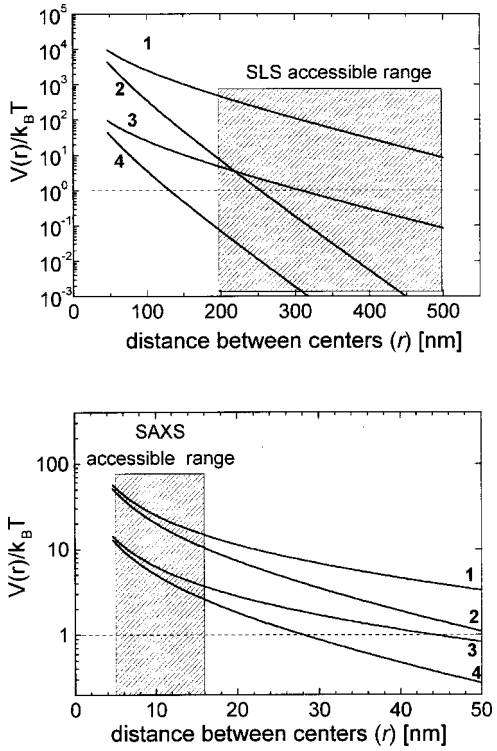

FIG. 7. (a) Electrostatic potential divided by k_BT as a function of the distance between spheres of radius 200 Å. (b) same as (a) for spheres of radius 20 Å. Calculations were performed for two values of ionic strength and two sets of particle charge. The shaded areas indicate the distances at which correlation peaks could be detected by SLS and SAXS. The numbers on the figures denote the following combinations of salt concentration and particle charge: (a) **1**—$C_s=10^{-5}M$, $Z=-1000$; **2**—$C_s=10^{-4}M$, $Z=-1000$; **3**—$C_s=10^{-5}M$, $Z=-100$; **4**—$C_s=10^{-4}M$, $Z=-100$; (b) **1**—$C_s=10^{-5}M$, $Z=-20$; **2**—$C_s=10^{-4}M$, $Z=-20$; **3**—$C_s=10^{-5}M$, $Z=-10$; **4**—$C_s=10^{-4}M$, $Z=-20$.

tance between the molecules at a given concentration ($d=1/c_N^{1/3}$). In Figs. 8 and 9, we show digitized results of a series of SLS measurements of Li and Reed[13] on proteoglycan monomers plotted next to our SAXS data on the 20-mer. Figure 8 shows the ''raw'' results (to compare the influence of the concentration on the amplitudes), and in Fig. 9 all peaks are normalized to 1 at the maximum (to compare the widths). Qualitatively similar behavior is exhibited in the two cases.

We are convinced that the SLS and SAXS results reflect the same property of polyelectrolyte solutions: strong local correlations revealed by the peak in the structure factor with maximum position corresponding to the average distance between molecules in solution. The strength of these local correlations as reflected in the peak amplitudes and widths is strongly dependent on the electrostatic forces; the position of the correlation peak appears to be relatively insensitive to the electrostatic forces at constant polymer concentration.

B. Dynamic light scattering—slow mode

As mentioned in I and in the Introduction, a slow mode is most important in the photon correlation spectroscopy time-correlation function at low added salt concentrations and at high oligonucleotide concentrations.

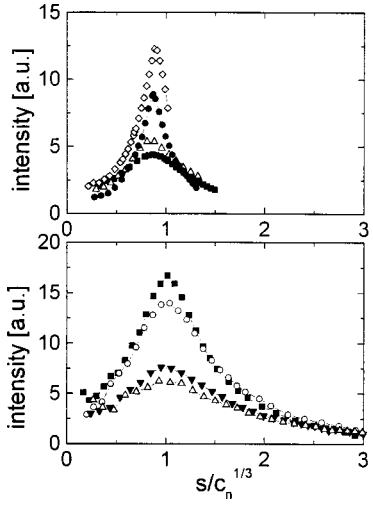

FIG. 8. Comparison of amplitudes of solution structure factors from SLS and SAXS at no added salt conditions. Top: light scattering data from Li and Reed. Bottom: SAXS data from the current work. Polymer concentration (from top to bottom): SLS—0.253, 0.12, 0.10, 0.08; SAXS—50, 30, 16.7, 12.6 mg/ml.

Figure 10 shows two correlation functions and their corresponding distribution of relaxation times obtained from CONTIN analysis. Note the large amplitude of the slow mode for the sample with no added salt. Figures 11 and 12 show the hydrodynamic radius and the relative amplitude of the slow mode determined from CONTIN and double exponential analyses measured at a scattering angle of 90 deg ($q=2.22\times10^5$ cm^{-1}). The relative amplitude of the slow mode peak in the double exponential analysis is defined as the amplitude of the slowly decaying exponential divided by the sum of the amplitudes of the fast and slowly decaying exponentials. In the CONTIN analysis, it is defined here as the area under the slow mode peak divided by the sum of the areas under the slow and fast mode peaks. The two methods of fitting gave the same results within the experimental error. Figure 11 shows the dependence on salt concentration of the relative

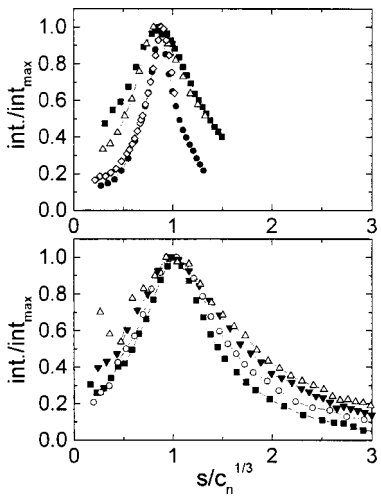

FIG. 9. Comparison of widths of solution structure factors from SLS and SAXS at no added salt conditions. Top: light-scattering data from Li and Reed. Bottom: SAXS data from the current work. Symbols are the same as in Fig. 8.

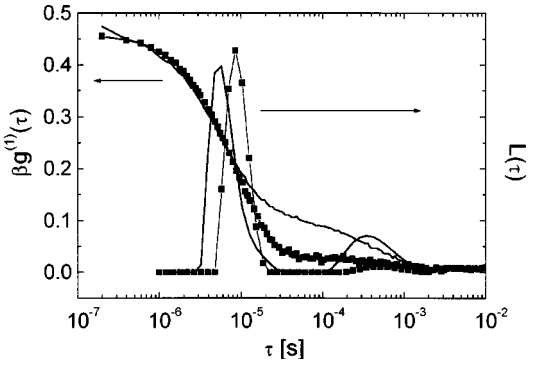

FIG. 10. DLS time correlations and CONTIN analysis at low (0 M, solid line) and high (100 mM, symbols) added salt, measured for the 20-mer at the concentration of 30 mg/ml.

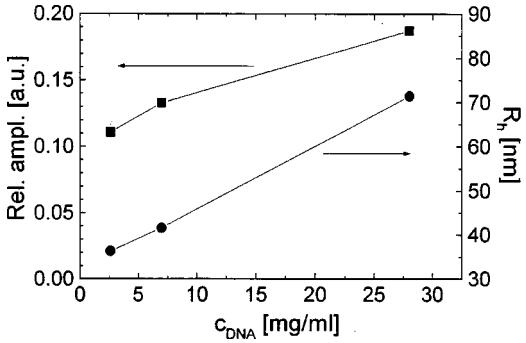

FIG. 12. Hydrodynamic radius and relative amplitude of the slow mode of the oligomer as a function of oligomer concentration for a constant salt concentration of 10 mM NaCl. Solid lines connecting points are meant to guide the eye.

amplitude and hydrodynamic radius for an oligonucleotide concentration of 10 mg/ml. As the salt concentration is lowered, the amplitude of the slow mode becomes about 22% of the total intensity while the hydrodynamic radius climbs close to 80 nm at the lowest salt concentration studied. The inset in Fig. 11 shows the dependence of the width of the SAXS peak (half-width at half-height) on salt concentration for the same 20-mer concentration. The SAXS peak width decreases as the amplitude and hydrodynamic radius of the slow mode increase—an indicator of a tightening of the local order.

Figure 12 shows the oligonucleotide concentration dependence for a constant added salt concentration of 10 mM NaCl. The slow mode amplitude increases with increasing DNA concentration and decreasing added salt concentration. In general, at high salt and low DNA concentration, the slow mode has a small amplitude and small hydrodynamic radius. As the added salt concentration decreases and the DNA concentration increases, the slow mode amplitude increases to about 40%, but never overwhelmingly dominates the CONTIN output.

Our CONTIN amplitudes correspond to the scattered light intensity distribution. This means that if the slow mode originates from large particles, stable aggregates, or ''temporal'' aggregates, the number density of those large particles or aggregates must be very small, since large particles normally scatter more light than smaller ones.

More polydisperse (but also longer DNA) samples were reported[5–7] to have a slow mode that dominates the CONTIN output. It has been suggested that the slow mode that is observed from polydisperse samples does not originate purely from the electrostatic or other long range interactions, but is related to interparticle (self-) diffusion. The current sample is not polydisperse, so this is not a plausible explanation of the slow mode in this system. In addition, Wang *et al.*[5] have measured the self diffusion coefficient for a larger, more polydisperse DNA by forced Rayleigh scattering, and have shown that it does not correspond to that derived from the slow mode in the dynamic light scattering photon correlation spectroscopy time correlation function. The small amplitude of the slow mode in the oligonucleotide case thus may, at least in part, be a reflection of the monodispersity of this carefully prepared sample. Our observations are generally consistent with those of Sedlak,[17] including the fact that our slow mode is present even at the highest salt concentrations studied.

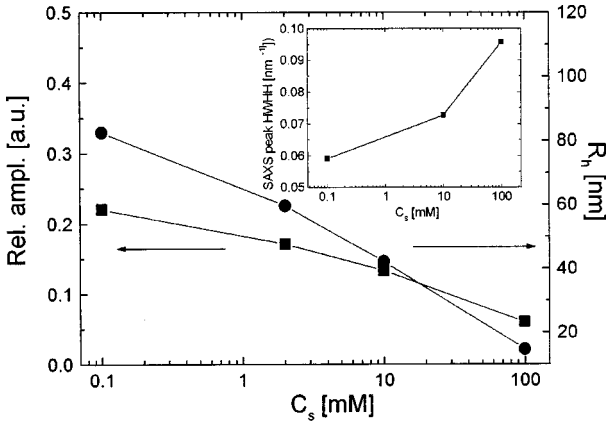

FIG. 11. Hydrodynamic radius and relative amplitude of the slow mode of the oligomer as a function of salt concentration for a constant oligomer concentration of 10 mg/ml. The inset shows the width of SAXS peaks (HWHH) vs salt concentration measured at the oligomer concentration of 30 mg/ml. Solid lines connecting points are meant to guide the eye.

We have, furthermore, performed a limited series of measurements of the slow mode absolute intensity at no added salt and an oligomer concentration of 10 mg/ml. A complication with these measurements is that the slow mode becomes multiexponential at low scattering angles. In any case, we lump the total intensity of these slow modes together. From plots of the reciprocal of this total intensity vs q^2, we obtain a radius of gyration of about 113 nm. The hydrodynamic radius obtained from the decay time of the slow mode is q dependent, increasing at low q to a value comparable to that given by the intensity measurements. These observations, although not conclusive, lend some support to the temporal aggregate view of the slow mode origin. More extensive measurements of this type are in progress.

A direct correlation between small angle neutron scattering and the slow mode has been seen for a concentrated DNA sonication fragment by Borsali *et al.*[10] These authors observed an ''upturn'' in the very low q region $[0.073 < q\ (\mathrm{nm}^{-1}) < 0.20]$ that was assigned to longer range correlations among the polyions. Analysis of the upturn by

Guinier methods gives an apparent radius of gyration. This radius of gyration was smaller than that obtained by the same authors using SLS, an indication that the neutron q used was not small enough to see the whole correlation volume. The x-ray apparatus used in this work could not attain the small q region necessary to observe any upturn that may have been present. The minimum q that could be reliably observed with our SAXS apparatus was 0.14 nm^{-1}.

IV. CONCLUSIONS

Our 20 base pair oligonucleotide system is essentially monodisperse, rigid, and rodlike. SAXS and dynamic light scattering (DLS) experiments on it are therefore not subject to many of the uncertainties in interpretation that have plagued the polyelectrolyte field for many years. Our analysis shows that both the SAXS peak and the slow mode are the result of interpolyion solution correlations that are strongly dependent on the electrostatic forces. The SAXS peaks reveal the nearest neighbor correlations while the DLS slow mode indicates longer range correlations, essentially a ''correlation volume.'' The hydrodynamic radius of the slow mode is q dependent at low salt. As pointed out by Sedlak,[17] the hydrodynamic radius does not necessarily correspond to the radius of the correlation volume. The slow mode could correspond to a temporal aggregate, and the ''diffusion coefficient'' associated with it could result from a more complex process than simple diffusion of the whole aggregate. Alternatively, if there is a distribution of temporal aggregates of different sizes and these live longer than the time it takes to diffuse a distance $1/q$, we expect a complex nonsingle exponential slow mode time correlation function. Single exponential fits to such a correlation function would give q-dependent hydrodynamic radii.

In our system, the slow mode and the SAXS peak are generally present together and appear to diminish in importance in a similar way as the salt concentration is increased. There is, however, a salt concentration above which the SAXS peak is too weak to observe, but the slow mode, although weak, is still observable.

In I, we showed that the coupled mode theory with charge renormalization via the counterion condensation theory gives good agreement with the photon correlation fast mode relaxation times. This approach is inadequate for the slow mode. The long range interpolyion correlations revealed by the slow mode experiments could result from the purely repulsive forces described in this article. There is, however, much speculation in the literature that there is also an effective attractive force between the polyions arising from fluctuations in the counterion positions that are not included in the mean field theories used here and in I. There is currently much activity devoted to resolving this and related issues.[27–31]

ACKNOWLEDGMENTS

This work was supported by National Science Foundation (USA) Grant No. CHE-9520845 to R.P., the US–Polish Marie Sklowdowska-Curie Joint Fund II Grant: MEN/NSF-96-254 and by the Volkswagen Stiftung, Federal Republic of Germany. We are grateful to Dr. Werner Steffen and Dr. Thomas Thurn-Albrecht for their help with the small-angle x-ray experiments.

[1] H. Liu, L. Skibinska, J. Gapinski, A. Patkowski, E. W. Fischer, and R. Pecora, J. Chem. Phys. **109**, 7556 (1998).
[2] A. W. Fulmer, J. A. Benbassat, and V. A. Bloomfield, Biopolymers **20**, 1147 (1981).
[3] K. S. Schmitz and M. Lu, Biopolymers **23**, 797 (1984).
[4] T. Nicolai and M. Mandel, Macromolecules **22**, 438 (); **22**, 2348 (1989).
[5] L. Wang, M. Garner, and H. Yu, Macromolecules **24**, 2368 (1991).
[6] H. Tj. Goinga and R. Pecora, Macromolecules **24**, 6128 (1991).
[7] M. E. Ferrari and V. A. Bloomfield, Macromolecules **25**, 5266 (1992).
[8] J. Newman, J. Tracy, and R. Pecora, Macromolecules **27**, 6808 (1994).
[9] P. Wissenburg, T. Odijk, P. Cirkel, and M. Mandel, Macromolecules **28**, 2315 (1995).
[10] R. Borsali, H. Nguyen, and R. Pecora, Macromolecules **31**, 1548 (1998).
[11] S. C. Lin, W. I. Lee, and J. M. Schurr, Biopolymers **17**, 1041 (1978).
[12] M. Drifford and J. P. Dalbiez, J. Phys. Chem. **88**, 5368 (1984).
[13] X. Li and W. F. Reed, J. Chem. Phys. **94**, 4568 (1991).
[14] S. Ghosh, R. M. Peitzsch, and W. F. Reed, Biopolymers **32**, 1105 (1992).
[15] M. Sedlak and E. Amis, J. Chem. Phys. **96**, 817 (1992).
[16] W. F. Reed, Macromolecules **27**, 873 (1994).
[17] M. Sedlak, J. Chem. Phys. **105**, 10123 (1996).
[18] A. Patkowski, E. Gulari, and B. Chu, J. Chem. Phys. **73**, 4178 (1980).
[19] L. Wang and V. A. Bloomfield, Macromolecules **24**, 5791 (1991).
[20] M. H. J. Koch, Z. Sayers, P. Sicre, and D. Svergun, Macromolecules **28**, 4904 (1995).
[21] I. Morfin, W. Reed, M. Rinaudo, and R. Borsali, J. Phys. II **4**, 1001 (1994).
[22] S. W. Provencher, Comput. Phys. Commun. **27**, 213 (); **27**, 229 (1982).
[23] R. Koyama, Macromolecules **17**, 1594 (1984); **19**, 178 (1986).
[24] J. Garcia de la Torre, S. Navarro, M. Lopez Martinez, F. Diaz, and J. Lopez Cascales, Biophys. J. **66**, 1573 (1994).
[25] F. Diaz, J. Lopez Cascales, and J. Garcia de la Torre, J. Biochem. Biophys. Methods **26**, 261 (1993).
[26] N. Ise, T. Okubo, S. Kunugi, H. Tomiyama, and Y. Yoshikawa, J. Chem. Phys. **81**, 3294 (1984).
[27] K. S. Schmitz, Langmuir **13**, 5849 (1997).
[28] M. Muthukumar, J. Chem. Phys. **107**, 2619 (1997).
[29] N. Gronbech-Jensen, R. J. Masl, R. F. Bruinsma, and W. M. Gelbart, Phys. Rev. Lett. **78**, 2477 (1997).
[30] B.-Y. Ha and A. Liu, Phys. Rev. Lett. **79**, 1289 (1997).
[31] R. Podgornik and V. A. Parsegian, Phys. Rev. Lett. **80**, 1560 (1998).
[32] M. Corti and V. Degiorgio, J. Phys. Chem. **85**, 711 (1981).